GSI

GSI-Preprint-98-67
Dezember 1998

HEAVY-ION REACTIONS AT THE GSI DARMSTADT

V.Metag

(Invited talk given at the Erice School on Nuclear Physics, Erice, Sicily, Italy, Sept. 17-25, 1998)

Gesellschaft für Schwerionenforschung mbH
Planckstraße 1 • D-64291 Darmstadt • Germany
Postfach 11 05 52 • D-64220 Darmstadt • Germany

Heavy-Ion Reactions at the GSI Darmstadt

VOLKER METAG

Gesellschaft für Schwerionenforschung, Darmstadt

and

II. Physikalisches Institut, Universität Gießen, Gießen

In nucleus-nucleus collisions at bombarding energies on the order of 1 AGeV nuclear matter can be compressed to similar densities as encountered in stellar processes, i.e. to 2-3 times normal density. Experimental data providing information on the space-time evolution of these collisions are presented: the properties of hadrons in the hot and compressed nuclear medium in the high-density phase, collective flow phenomena during the expansion phase, and the hadrochemical composition of the collision system in the final stage of the reaction at freeze-out are discussed. Future directions in the heavy-ion reaction program are indicated.

1 Introduction

Collisions of relativistic heavy ions provide a unique approach to study the compression and excitation of nuclear matter. According to various theoretical descriptions [1, 2, 3] nucleon densities up to 3 times normal nuclear matter density are reached in the reaction volume at incident energies of about 2 AGeV. The space-time evolution of the reaction is illustrated in a simulation shown in fig. 1. Two nuclei collide with a relative velocity of $\approx$ 90 % light velocity. In a sequence of nucleon-nucleon collisions nuclear

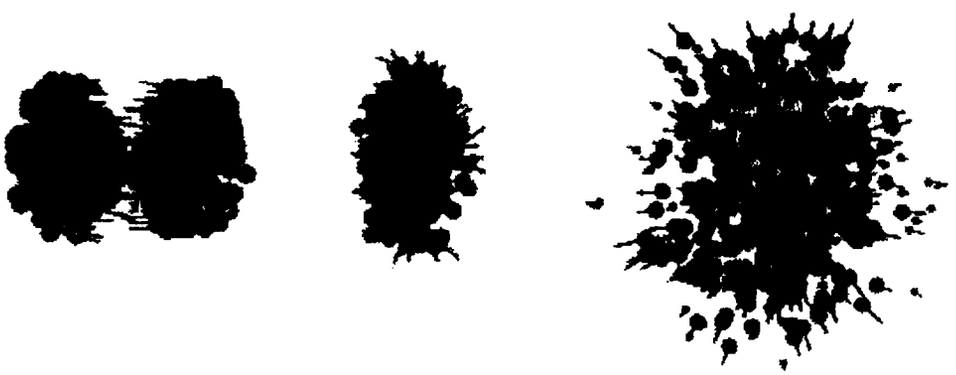

Figure 1: Space-time evolution (3 snap shots separated by time steps of $\approx 10 fm/c = 3 \cdot 10^{-23} s$) of a central nucleus-nucleus collision (Au+Au at 2 AGeV) simulated within the IQMD-model [4].

matter is stopped and compressed. Finally, the pressure built up in the reaction zone is released by an expansion of the collision system. The main experimental question is whether there are observables which are specific for each of the various reaction phases, in particular for the high-density phase. Are

there signals from the compressed nuclear matter which are not masked or distorted in the later lower density stages of the collision?

During the compression phase, a fraction of the initial kinetic energy in the collision system is converted into the intrinsic degrees of freedom of the nucleons, leading to the excitation of baryon resonances which subsequently decay by meson emission. The abundance and spectral distributions of the mesons are thus an important information which, however, suffers in most cases from secondary interactions of the mesons. A more direct view of the high-density collision zone is provided by dileptons which are not subject to strong final state interactions. In particular, the e^+e^- decays of ρ, ω, and ϕ mesons are sensitive to possible modifications of these vector mesons within the medium which may be associated with a partial restoration of chiral symmetry at high baryon densities. It should be noted, however, that also these signals may be distorted by dilepton emission in later stages of the reaction.

The pressure built up in the compressed collision zone is released by an expansion of the system. Collective flow phenomena such as directed sideward flow, elliptic flow, and radial flow have been observed and related to the equation-of-state of nuclear matter.

When during the expansion the spacing among hadrons has become so large that interactions among them have ceased the hadrochemical composition of the system is frozen. If chemical equilibrium has been achieved by this stage, then the measured particle production ratios can be used in a thermal model analysis to determine the temperature and chemical potential of the system at freeze-out. This provides lower bounds for the densities and temperatures reached during the high-density phase of the reaction.

In the following chapters the various phenomena will be discussed in time reversed order.

2 The Freeze-Out Phase

In the course of a heavy-ion reaction many nucleon-nucleon collisions occur which are energetic enough to excite the intrinsic degrees of freedom of the nucleons. As any composite system the nucleon exhibits a rich excitation energy spectrum with broad ($\Gamma \approx 100$ MeV) resonance states which decay primarily by meson ($\pi, \eta, K, \omega ...$) emission to the nucleon ground state. The study of meson production is thus the appropriate approach to learn more about the conversion of the initial kinetic energy of the two colliding nuclei into internal excitations. π emission from the lowest, non-strange excited state of the nucleon, the $\Delta(1232)$ resonance, is the predominant source of pions in heavy-ion reactions at SIS energies. Higher lying, mostly overlapping resonances also emit pions but are less frequently populated. The η meson plays a special role as it is a selective probe for the excitation of the $S_{11}(1535)$ resonance which is the only baryon resonance with a sizable (≈ 50 %) η branching ratio. After the

initial production, mesons propagate through the collision zone, i.e. they are rescattered or absorbed and re-emitted, as described e.g., in [5, 6]. As a result of this series of absorption and re-emission processes an equilibrium population of the various hadron species may evolve which is frozen when - due to the expansion of the collision system - particle species changing (i.e. inelastic) reactions die out with the increasing spacing among the hadrons. At this freeze-out point, a thermal model analysis of the hadrochemical composition of the collision system may become viable, providing information on global properties of the nuclear medium such as freeze-out temperatures and -densities.

Meson production in heavy-ion collisions has been studied over a wide energy and mass range. Resulting production probabilities per participant nucleon are shown in fig. 2 as a function of the available energy per nucleon-nucleon pair. To allow for a comparison of different particle species the available energy is divided by the mass of the respective particle [7]. The production probabilities for pions and η mesons fall close to one curve over 4 orders of magnitude. In contrast, K^+- and K^-

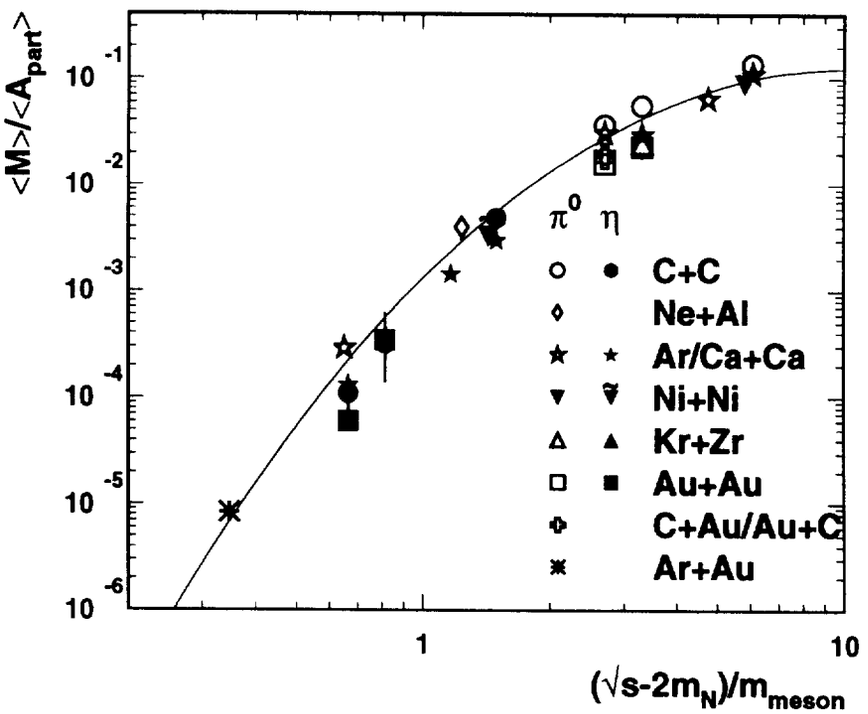

Figure 2: Meson production probability per participant nucleon as a function of the available energy normalized to the meson mass. The figure has been prepared by R. Averbeck [7].

production probabilities (not shown in fig. 2) are down by up to a factor 5 compared to π, η production. This may indicate that the strangeness degree of freedom is not fully equilibrated at SIS energies, in particular because of the long mean free path of K^+ mesons. (see, however, the discussion in [8]).

Assuming an equilibrated, pion and η meson emitting system, its hadrochemical composition can be analyzed within a thermal model. Following the work of Braun-Munzinger et al. [9], the system at chemical freeze out is regarded as a hadron gas consisting of $\pi, \eta, N, \Delta(1232), N^*(1440), N^*(1535)$,

higher lying baryon resonances, and deuterons in chemical and thermal equilibrium; the density of each constituent is then given by two parameters, the temperature T and the baryochemical potential μ_B:

$$\rho(\mu_B, T) = \frac{g}{(2\pi\hbar)^3} \int 4\pi p^2 f(pR) dp \int \frac{A(m) dm}{\exp[(E - \mu_B B)/T] \pm 1} \tag{1}$$

where g is the spin-isospin degeneracy, A(m) the resonance mass distribution and f(pR) a finite volume correction. The $\pm$ sign refers to the different statistics for fermions and bosons, respectively.

From the π^0 production probability per participant nucleon $\pi^0 / < A_{part} >$, the production ratio η/π^0 [7], and the production rates of π, Δ, p, d [10] the paramteres μ_B and T have been determined for different collision systems and bombarding energies using eq. (1). The results are included in the phase diagram of hadronic matter shown in fig. 3 which also contains (T,μ_B)-determinations from

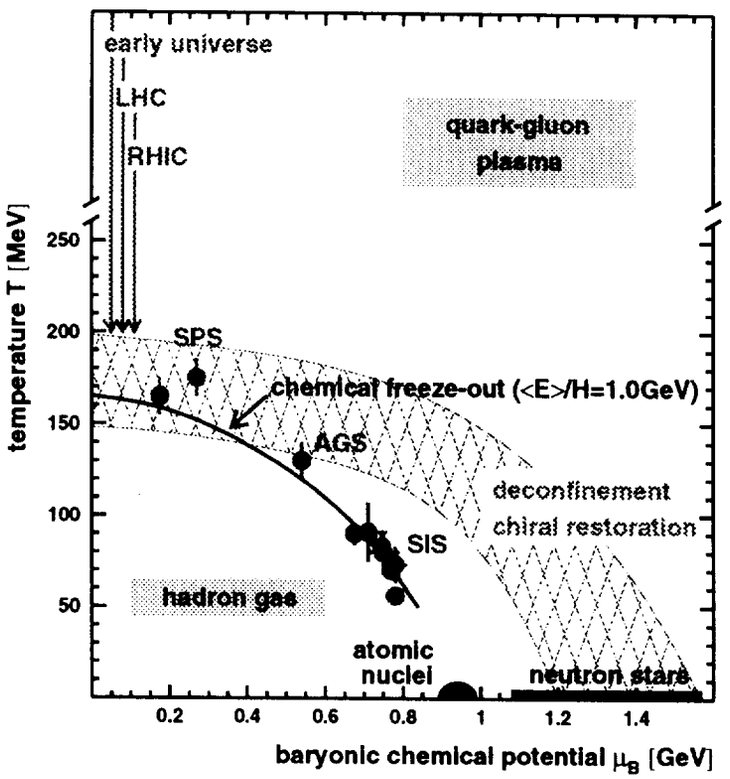

Figure 3: Phase diagram of hadronic matter; temperatures T and baryochemical potential μ_B derived from particle production ratios in nucleus-nucleus reactions are plotted for different bombarding energies [7, 9, 10, 11]. The solid curve through these data points represents the curve for chemical freeze-out of hadronic matter as discussed in [12].

particle production experiments at AGS and SPS energies [9, 11]. The data points are connected by the (chemical) freeze out curve for hadronic matter which - as recently noticed by Cleymans and Redlich [12] - is close to an energy per hadron of 1 GeV.

It is evident that - if equilibrium is really achieved - these parameter values determined at freeze-out can only be lower bounds for the temperatures and densities reached in the high-density phase of the reaction. Having this in mind, it is even more remarkable that for AGS and SPS energies the collision system at freeze out is near the phase transition to the quark-gluon-plasma.

3 The Expansion Phase: collective phenomena in nucleus - nucleus collisions

The quest for collective phenomena has been a crucial aspect in the study of heavy-ion reactions since the very beginning: are nucleus-nucleus collisions a sequence of more or less independent nucleon-nucleon collisions proceeding in parallel or are there qualitatively new features of collective character? In the following, the experimental results on flow phenomena are summarized.

3.1 Azimuthal anisotropy and Directed Flow

Historically, the first collective effect established in heavy-ion reactions was the directed sideward flow observed in non-central collisions [13]. Here, the incomplete geometrical overlap of target and projectile nuclei defines a reaction plane and introduces an in-plane/out-of-plane asymmetry. The spectators which do not experience first chance collisions are deflected sideways by the expanding collision zone and by repulsive field gradients at the border between participant and spectator matter [14]. While this phenomenon gives rise to a preferential in-plane emission of nucleons, another azimuthal asymmetry may arise from spectator nucleons blocking the path of participant nucleons and/or produced mesons (shadowing) which leads to a squeeze-out of hadronic matter preferentially perpendicular to the reaction plane.

These azimuthal anisotropies can be quantitatively described by the following Fourier series [15, 16]

$$F(\Phi) = F_0(1 + \sum_i 2v_i cos(i\Phi)) \tag{2}$$

where the coefficients v_1, v_2 are denoted as 'directed flow' and 'elliptic flow', respectively.

The squeeze-out of hadronic matter perpendicular to the reaction plane, as observed at BEVALAC and SIS energies, is characterized by a negative v_2 coefficient. At higher energies (see fig. 4), the interaction times of projectile and target nuclei are so short that the shadowing effect is reduced and the compressed collision zone can preferentially expand within the reaction plane, giving rise to positive elliptic flow.

It has recently been argued [17] that the change in sign of elliptic flow as a function of incident energy is particularly sensitive to a softening of the equation-of-state of hadronic matter which might

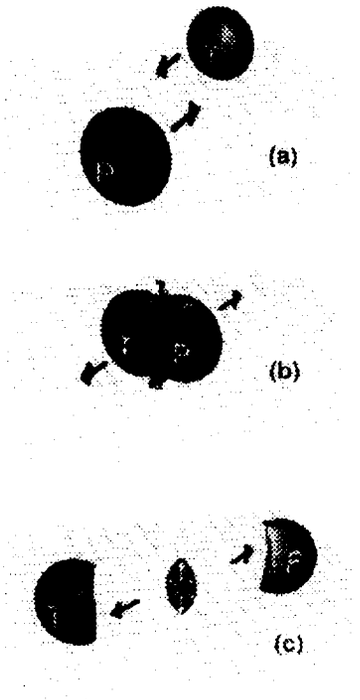

Figure 4: Schematic illustration of elliptic flow in a non-central heavy-ion collision at relativistic energies; (a) projectile and target nucleus approach each other at a certain impact parameter, (b) squeeze-out of nuclear matter and produced particles perpendicular to the reaction plane (negative elliptic flow) due to shadowing, (c) late stage of the collision: expansion of the compressed collision zone within the reaction plane (positive elliptic flow). The figure is taken from [17].

be expected near the phase transition to the quark-gluon-plasma. Recent results from the E895 collaboration at the AGS together with earlier data on elliptic flow obtained at the AGS and SPS will allow a quantitative comparison to these theoretical predictions.

3.2 Collective radial flow

An important discovery at GSI has been the observation of an azimuthally symmetric, radial flow in central nucleus-nucleus collisions [18] where a reaction plane can no longer be defined and the axial symmetry of the problem ideally gives rise to a Φ-symmetric emission pattern. Experimentally, this phenomenon could only be established after methods of selecting central collisions had been refined by, e.g. requiring a high degree of azimuthal symmetry in the event topology

The observed expansion of the collision zone has turned out to be a superposition of a collective and a thermal motion. If the radial expansion were purely collective, all particles - irrespective of their mass - would move with the same local *flow* velocity, i.e. the total kinetic energy is proportional to the particle mass: $E_{kin} = A\frac{m_0 v^2}{2}$ or $\epsilon_{coll} = \frac{E_{kin}}{A} = \text{const}$. For thermal motion, the kinetic energy is proportional to the temperature T, i.e. $E_{kin} \sim T$. A superposition of both types of motion will give rise to a mass dependence $E_{kin} \sim T + \epsilon_{coll} \cdot A$, as experimentally observed (see fig. 5). Systematic studies by the FOPI [14] and EOS [19] collaborations for a large number of collision systems and bombarding energies [20] (see Fig. 6) have revealed an increase of the transverse expansion velocity β_t reaching $\approx$ 35 % of the velocity of light at 2 A GeV. This implies that - depending on the incident energy - 20

to 50 % of the initially available kinetic energy is converted into this collective expansion in the SIS

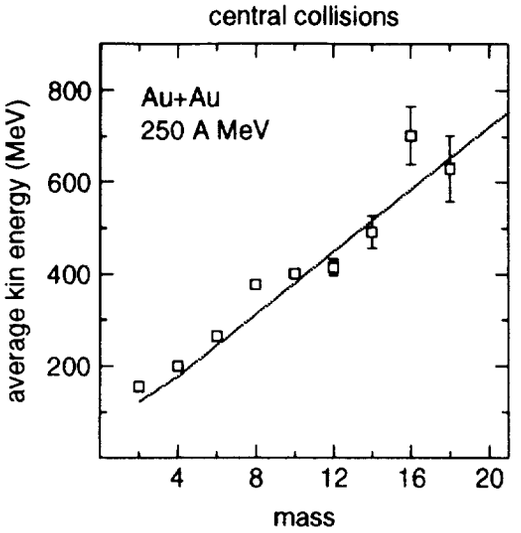

Figure 5: Average kinetic energy of nuclear fragments as a function of fragment mass for central Au-Au collisions at 250 AMeV. The figure is taken from ref. [14].

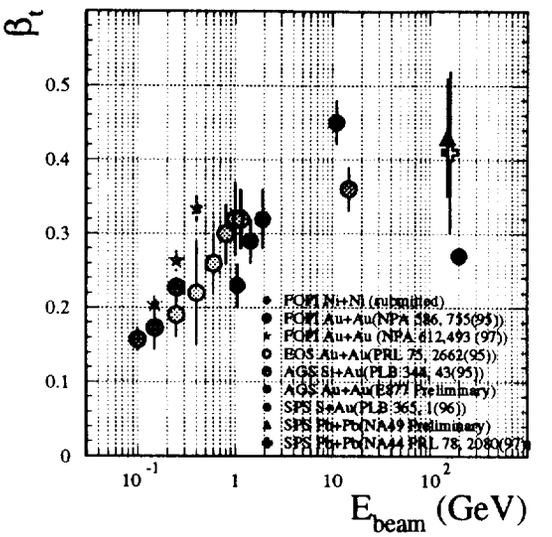

Figure 6: Systematics of transverse flow velocities for different collision systems and bombarding energies. The data have been compiled by N. Herrmann from refs. [9, 11, 14, 20, 19, 21, 22].

energy regime. For higher energies, AGS and SPS experiments [9, 11, 21, 22] indicate a saturation at around $\beta_t \approx 0.4$c.

4 The High-Density Phase

Although very short lived ($\tau \approx 10 fm/c$), the high-density phase of the reaction may provide important information on the properties of hadrons in compressed nuclear matter. Recent theoretical studies by several groups [23, 24] predict changes in mass and width of hadrons when embedded in nuclear matter even at normal density. Experimental and theoretical investigations of this kind may thus help to unreval the origin of mass of bound hadronic systems. In some model calculations the changes in hadron properties are associated with a partial restoration of chiral symmetry with increasing baryon density and temperature, parameters which can be varied and controlled in heavy-ion reactions by choosing appropriate beam energies and sizes of collision systems. These ideas have stimulated an active research program at GSI and other heavy-ion laboratories. In the following, the current status on mass modifications is discussed separately for pseudoscalar and vector mesons.

4.1 Pseudoscalar mesons in the nuclear medium

In the nuclear medium, the low energy interactions of kaons are governed by theorems based on chiral dynamics. This has an impact on K production and propagation in heavy-ion reactions. Starting from effective chiral perturbation theory, an in-medium dispersion relation for kaons can be derived [25, 26, 27, 28]. The total energy of the kaons is not only given by the K mass and the momentum as for free kaons but there are additional terms due to the interaction of kaons with the medium:

$$\omega_K^{\pm}(p,\rho_b) = \sqrt{m_K^2 + p^2 - \frac{\Sigma_{KN}}{f_K^2}\rho_s + (\frac{3\rho_B}{8f_K^2})^2} \pm \frac{3\rho_B}{8f_K^2} = U_s + U_v + \sqrt{m_K^2 + p^2} = \sqrt{m_K^{*2} + p^2} \qquad (3)$$

The additional terms can be re-written as a scalar and a vector potential or they can be absorbed into effective kaon masses. Because of the different signs of the additional terms, the effective masses of K^+ and K^- mesons behave differently as a function of baryon density (see fig.7). While the effective

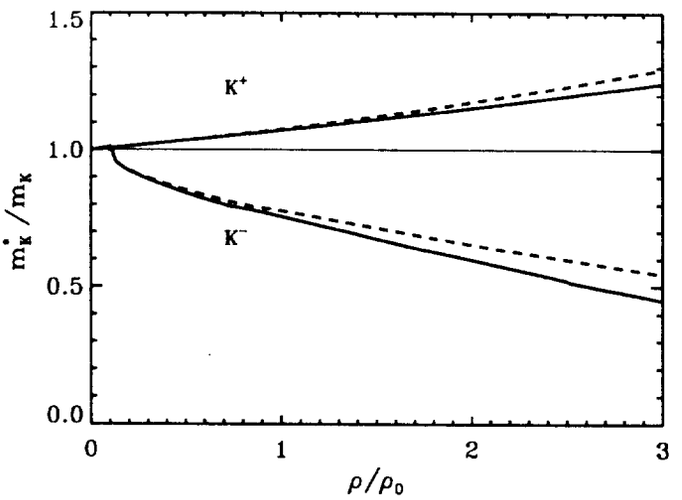

Figure 7: Ratio of effective to free masses of K^+ and K^- mesons in symmetric nuclear matter as a function of the baryon density ρ in units of the normal nuclear matter density ρ_0. The figure is taken from ref. [26]. The solid curves include Pauli blocking, binding, and Fermi motion while the dashed curves show the additional effects of nucleon-nucleon correlations [27].

K^+ mass varies only little with baryon density, a dramatic decrease in the K^- mass is predicted, dropping to about 50 to 60 % of the free K mass at 2.5 times normal nuclear matter density [26] which can be reached in central collisions at SIS energies. An experimentally observable consequence of a reduced K^- mass would be an enhanced K^- yield as it would be energetically much easier to produce K^- mesons in dense hadronic matter; when leaving the collision zone, kaons acquire their free mass from the total energy of the system. In addition, once the kaons are produced in the medium, their propagation is subject to the additional potentials which will act on them. This leads to a specific flow behaviour [29, 30]. Both these theoretical predictions have been tested experimentally at GSI.

Elementary reactions, in particular those recently measured at COSY (see fig.8a) [31, 32], show that at the same energy above threshold the cross section for K^+ production in proton-proton reactions is at least an order of magnitude larger than for K^- production over a wide energy range. If one selects

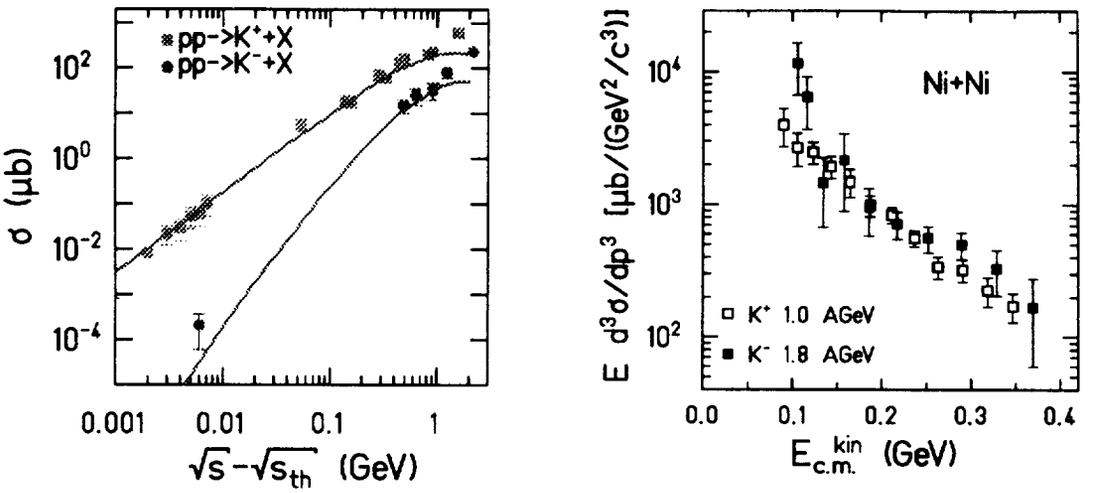

Figure 8: Cross sections for K^+ and K^- production in p-p (a:left) and Ni-Ni (b:right) reactions. The incident energies for the nucleus-nucleus reactions correspond to the same energy below the nucleon-nucleon production threshold. The figure is taken from [33].

the same energy below threshold in a heavy-ion reaction the K^+ and K^- yields are equal, as shown in fig.8b [33]. In view of the difference in the elementary cross sections and because of the expected strong absorption of K^- mesons in nuclei, the observation of equal cross sections for K^+ and K^- mesons in nucleus-nucleus collisions rather implies a strong K^- enhancement. Since secondary reactions like $\pi^-\Lambda \rightarrow nK^-$ are found not to account for the observed K^- yield [34], the measured K^- enhancement may be regarded as some first tentative evidence for K mass modification in the dense medium.

According to theoretical predictions, the propagation of kaons in the collision zone is governed by the additional scalar and vector potentials. In non-central heavy-ion collisions, nucleons flow sidewards pushed by the exploding collision zone (see 3.1). Although kaons and Λ's are produced in associated production at the same point in space and time within the collision zone, the propagation of kaons in the medium is obviously completely different from that of Λ's. The Λ's flow with the nucleons as shown in the upper half of fig. 4.1 where the average transverse momentum projected onto the reaction plane is plotted for protons and Λ's as a function of scaled rapidity [35]. Below, the same quantity is shown for kaons which exhibit almost no flow, i.e. the average transverse momentum projected on the reaction plane is ≈ 0. This difference can be ascribed to the action of additional potentials. Transport model calculations including scalar and vector potentials acting on kaons do indeed reproduce the experimental observation [34, 36].

At this point we can conclude that the experimental investigation of kaon production and propagation in relativistic nucleus-nuicleus collisions has provided intriguing results consistent with the

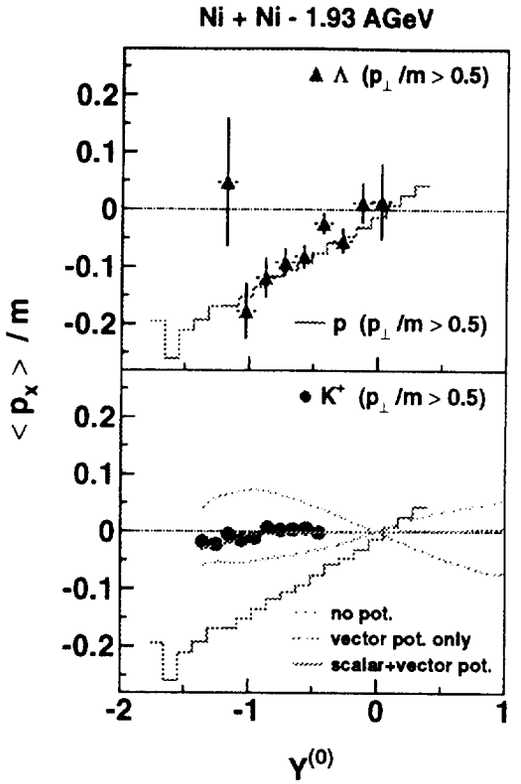

Figure 9: Directed sideward flow for protons, lambdas and kaons: the average transverse momentum projected onto the reaction plane is plotted as a function of the normalized rapidity [35]. $Y^{(0)}$ = -1, 0, 1 refer to target-, mid-, and projectile rapidity, respectively.

scenario of medium modifications as predicted theoretically by chiral dynamics. More detailed results on kaon production and propagation are discussed by N. Herrmann [37] and P. Senger [38].

4.2 Vector mesons in nuclear matter

There are various theoretical predictions that chiral symmetry may be restored with increasing baryon density and temperature which may lead to a dropping of vector meson masses in compressed hadronic matter [39].

At normal nuclear matter density and zero temperature nucleons are spaced at an average distance of about 1.8 fm which results in an average density of 0.17 nucleons per fm^3. The nucleons are surrounded by the QCD-vacuum which is not empty but densely populated by virtual scalar quark - antiquark pairs; this can be expressed by the chiral condensate with an expectation value about ten times higher than normal nuclear matter density. Inside nucleons chiral symmety is locally restored. When compressing nuclear matter, a given volume is filled with more and more nucleons and thereby the chiral condensate is reduced within this volume. Consequently, the chiral condensate drops with increasing baryon density. This is a rather pictorial description of what has been calculated [26] within the Nambu Jona-Lasinio model. Fig. 10 shows the chiral condensate as a function of baryon density and temperature. Parameter ranges where sizable changes in the chiral condensate are expected are accessible at different accelerators by using photon-, pion- and heavy-ion beams.

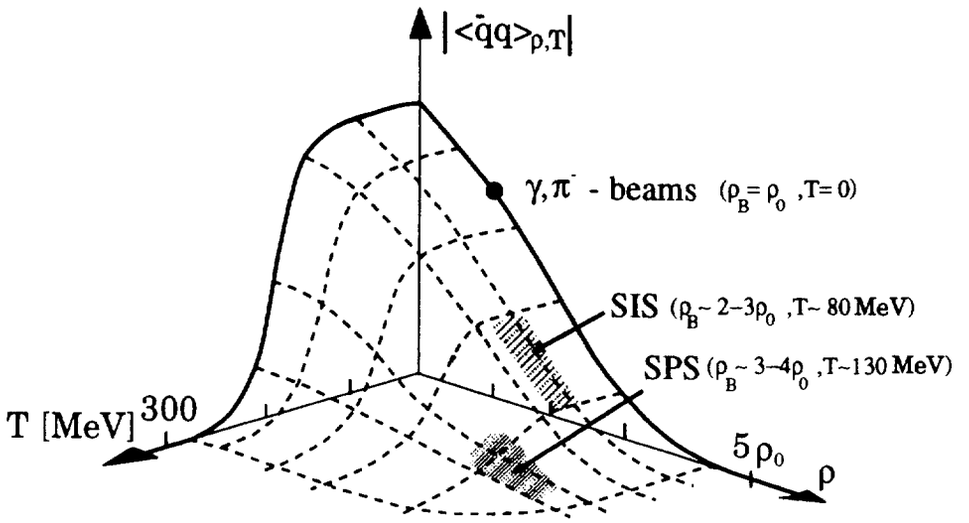

Figure 10: The chiral condensate calculated within the Nambu Jona-Lasinio model as a function of temperature and baryon density [23].

Are there any experimentally observable consequences? Theoretical predictions [26, 29, 39, 40] that vector meson masses should drop with the decreasing condensate can be tested experimentally. The best way to measure vector meson masses is to reconstruct their mass from their decay into e^+e^- pairs since the 4-momentum vectors of leptons are not changed by strong final-state interactions. Furthermore, vector mesons are sufficiently shortlived so that a considerable fraction will decay within the lifetime of the compressed collision zone.

Several experiments are already addressing this question. As an example, fig. 11 shows results of the DLS spectrometer [41] at the BEVALAC and the CERES detector [42] at CERN. The measured invariant mass spectra are compared to calculations [43] which allow for medium modifications of the ρ meson, implemented by a density dependent spectral function [44]. Although the calculations reproduce the data from the Pb + Au reaction at 160 AGeV, they underpredict the experimental results for Ca+Ca at 1 AGeV by up to a factor 3. (This excess is not observed for the p+p data below 2 GeV [45, 46] and increases with the mass of the collision system from p+d to Ca+Ca.)

For an interpretation of the spectra it is important to know at what time and baryon density the e^+e^- pairs are emitted. Contributions from the Dalitz decay of π^0 and η mesons ($\pi^0, \eta \rightarrow \gamma e^+e^-$) are delayed since the lifetimes of these pseudoscalar mesons are several orders of magnitude longer than the collision time. Their contribution can be subtracted from the measured e^+e^- spectrum provided π^0 and η yields have been measured for the specific collision system in other experiments. This is the case for Ar+Ca at 1 AGeV (see fig. 12) where π^0 and η production was studied via the 2 γ decay using the photon spectrometer TAPS [47, 48]. After subtracting this delayed component [48], a spectrum of the e^+e^- pairs emitted on the time scale of the collision system is obtained (see fig. 13). Are these

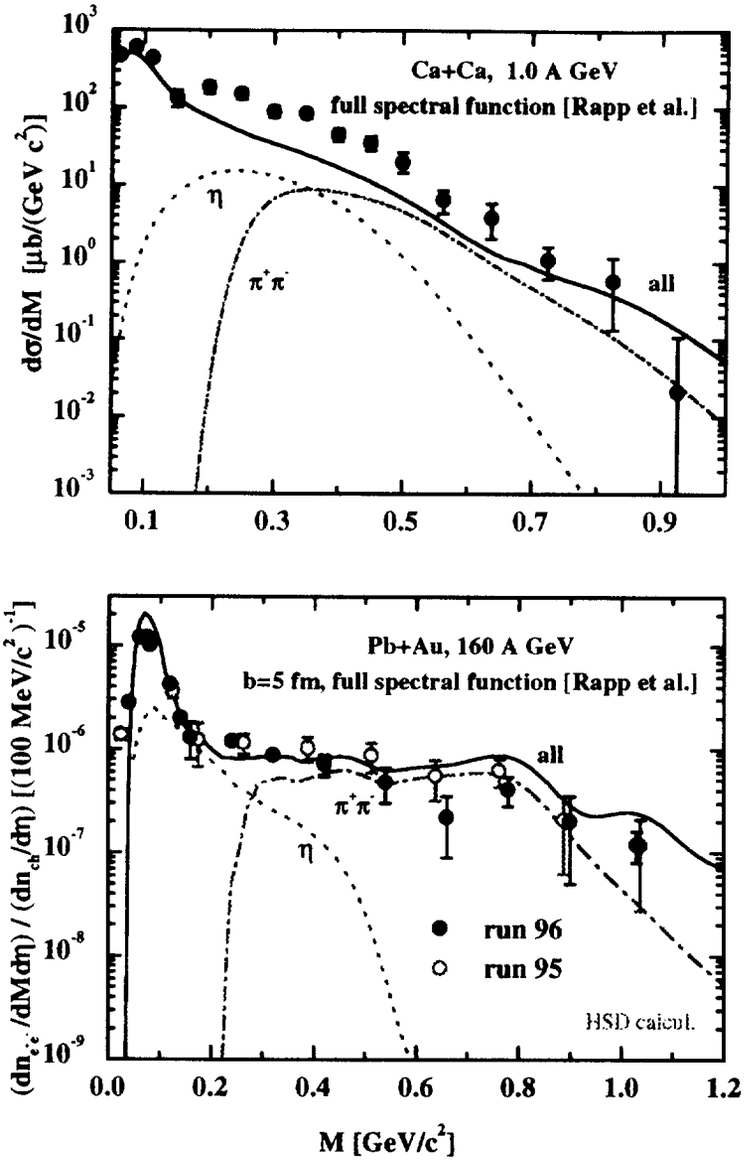

Figure 11: e^+e^- invariant mass spectra observed with the DLS spectrometer at the BEVALAC (upper frame) for Ca+Ca collisions at 1 AGeV [41] and with the CERES detector at the SPS (lower frame) in 160 AGeV Pb + Au collisions[42]. The data points are compared to calculations [43] which assume medium modifications of the ρ meson. Above 300 MeV/c^2, the contributions from $\pi^+\pi^- \rightarrow \rho \rightarrow e^+e^-$ annihilation appear to be dominant.

dileptons signals from the high-density phase of the reaction?

According to the calculations by Bratkovskaya et al. [43], a large fraction of the observed dilepton yield originates from $\pi^+\pi^- \rightarrow \rho \rightarrow e^+e^-$ annihilation which occurs, however, not only in the high baryon density phase but also later during the expansion of the collision system. Unfortunately, the dilepton spectrum is therefore **not specific** of the high-density phase of the reaction, as initially anticipated. It is nevertheless hoped that signals from $\omega, \Phi \rightarrow e^+e^-$ may maintain the information

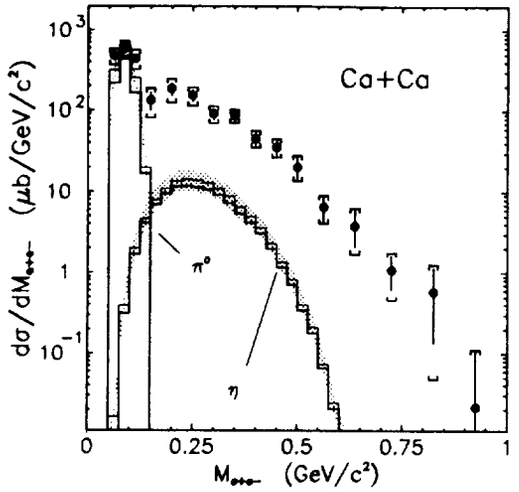

Figure 12: Measured e^+e^- invariant mass spectrum at 1 AGeV Ca+Ca [41]. The contribution of e^+e^- pairs from π^0 and η Dalitz decays derived from measured meson production cross sections [47, 48] is shown for comparison.

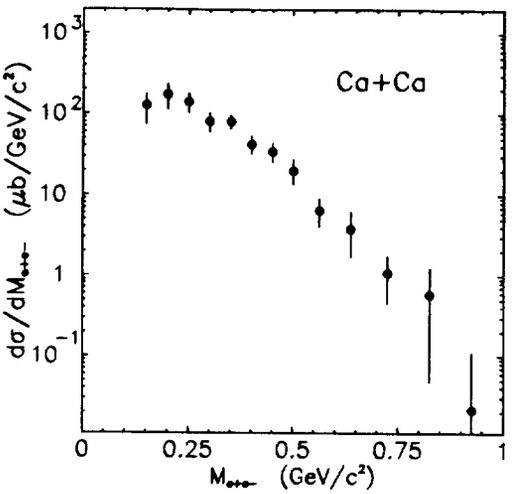

Figure 13: The dilepton spectrum of fig. 12 after subtraction of the delayed Dalitz decay contributions from π^0 and η mesons. The figure has been prepared by R. Holzmann.

from the initial high-density phase of the reaction. Their partial width for e^+e^-decay is, however, smaller than for the ρ meson and their contribution to the e^+e^- spectrum is consequently only a weak signal which requires high-resolution spectroscopy. The present data are insufficient, therefore a corresponding upgrade of the CERES detector has been implemented. At GSI, a large acceptance dilepton spectrometer HADES [49] is being installed by a European collaboration which will take up the challenge of high-resolution ($\delta m/m \approx 1\%$) dilepton spectroscopy in the 1 AGeV energy range.

In view of the problem that in heavy-ion reactions one studies dilepton emission from the full space-time history of the collision, involving high as well as low baryon densities, it is of particular importance that ω and Φ masses at normal nuclear matter density can be measured with HADES, exploiting the recently installed π -beam at GSI.

By choosing specific kinematical conditions, the $\pi^- p \rightarrow n\ \omega, \Phi$ reaction allows almost recoilless ω and Φ production to be studied which ensures that a large fraction of the vector mesons decay into lepton pairs within the nuclear medium. These measurements will constitute a crucial test of the various theoretical scenarios presently under discussion. Figs. 14 shows the available π-beam intensities and momenta, and fig. 15 shows the various meson species which can be produced.

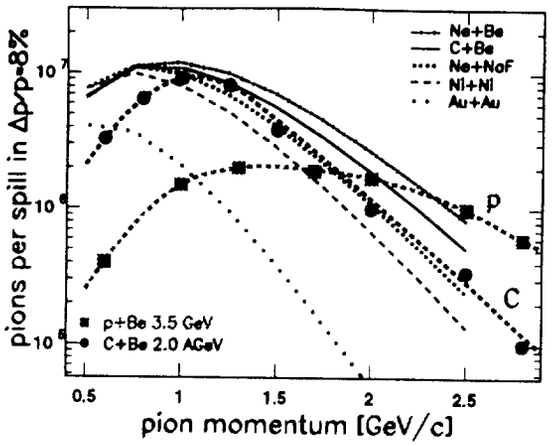

Figure 14: Pion intensity per spill at the HADES target position as a function of the π momentum, using primary carbon and proton beams at maximum intensity, respectively, in comparison to simulations for various projectile-target combinations.

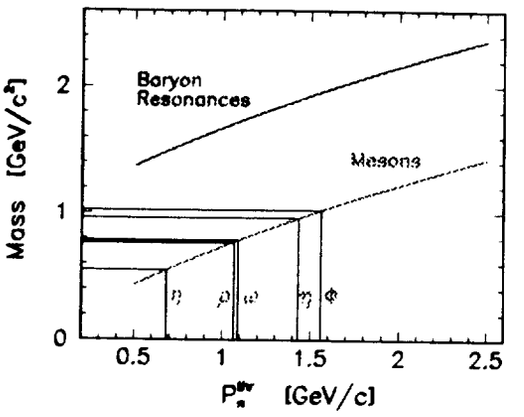

Figure 15: Minimum pion momentum for producing mesons or baryons of a given mass. [50].

5 Conclusions

Experimental results on the space-time evolution of relativistic heavy-ion collisions in the SIS energy regime have been discussed. Data on kaon production and propagation may be interpreted as first indications for medium-modifications of pseudoscalar mesons in the high-density phase of the reaction. Dilepton spectra may reflect in-medium changes in spectral functions of vector mesons; the bulk of the dilepton spectrum is, however, not sensitive to the highest baryon densities. Collective phenomena such as directed sideward flow, elliptic flow and radial expansion of the collision zone have been systematically studied as a function of incident energy and mass of the collision system. These studies are motivated by renewed theoretical attempts to relate these observables to the equation-of-state of nuclear matter. A rather consistent picture on freeze-out temperatures and baryon densities emerges from thermal model analyses of particle production ratios in the end-phase of the reaction for different bombarding energy regimes ranging from 0.5 to 160 AGeV.

It is a pleasure to acknowledge discussions with many colleagues, in particular with R. Averbeck, E. Bratkovskaya, P. Braun-Munzinger, W. Cassing, B. Friman, N. Herrmann, R. Holzmann, W. Kühn, U. Mosel, H. Oeschler, K. Redlich, W. Reisdorf, J. Ritman, P. Senger, H.J. Specht, J. Wambach and W. Weise.

References

[1] J. Aichelin, Phys. Rep. 202 (1991) 223

[2] W. Cassing *et al.*, Phys. Rep. 188 (1990) 363

[3] H. Stöcker and W. Greiner, Phys. Rep. 137 (1986) 277

[4] S. Bass, *et al.*, Phys. Lett. B335 (1994) 289 and private communication

[5] S. Bass *et al.*, Phys. Rev. C51 (1995) 3343

[6] P. Danielewicz, Phys. Rev. C51 (1995) 716

[7] R. Averbeck, nucl-ex/9803001

[8] J. Cleymans, H. Oeschler and K. Redlich, GSI-Preprint 98-59

[9] P. Braun-Munzinger *et al.*, Phys. Lett. B344 (1995) 43 and Phys. Lett B365 (1996) 1

[10] B. Hong *et al.*, Phys. Lett. B407 (1997) 115

[11] R. Stock *et al.*, Nucl. Phys. A630 (1998) 535c

[12] J. Cleymans and K. Redlich, GSI-Preprint 98-43

[13] H.A. Gustafsson *et al.*, Phys. Rev. Lett. 52 (1984) 1590

[14] W. Reisdorf *et al.*, Nucl. Phys. A612 (1997) 493

[15] P. Braun-Munzinger and J. Stachel, Nucl. Phys. A638 (1998) 3c

[16] J.Y. Ollitrault, Nucl. Phys. A638 (1998) 195c

[17] P. Danielewicz *et al.*, nucl-th/9803047

[18] S.C. Jeong *et al.*, Phys. Rev. Lett. 72 (1994) 3468

[19] M.A. Lisa *et al.*, Phys. Rev. Lett. 75 (1995) 2662

[20] W. Reisdorf and H.G. Ritter, Ann. Rev. Nucl. Part. Sci. 47 (1997) 663

[21] J. Stachel, Nucl. Phys. A610 (1996) 509c

[22] I.G. Bearden *et al.*, Phys. Rev. Lett. 78 (1997) 2080

[23] S. Klimt *et al.*, Phys. Lett. B249 (1990) 386

[24] M. Herrmann, B. L. Friman, and W. Nörenberg, Z. Phys. A343 (1992) 119

[25] A.E. Nelson and D. Kaplan, Phys. Lett. B192 (1987) 193

[26] W. Weise, Nucl. Phys. A 553 (1993) 59c

[27] T. Waas *et al.*, Phys. Lett. B379 (1996) 34 and Nucl. Phys. A617 (1997) 449

[28] J. Schaffner-Bielich *et al.*, Nucl. Phys. A625 (1997) 325

[29] G.Q. Li *et al.*, Phys. Rev. Lett. 79 (1997) 5214

[30] C.M. Ko and G.Q. Li, J. Phys.G: Nucl. Part. Phys. 22 (1996) 1673

[31] J.T. Balewski *et al.*, Phys. Lett. B338 (1996) 859

[32] J.T. Bilger *et al.*, Phys. Lett. B420 (1998) 217

[33] R. Barth *et al.*, Phys. Rev. Lett. 79 (1997) 4007

[34] W. Cassing *et al.*, Nucl. Phys. A614 (1997) 415

[35] J.L. Ritman *et al.*, Z. Phys. A352 (1995) 355

[36] E.L. Bratkovskaya *et al.*, Nucl. Phys. A622 (1997) 593

[37] N. Herrmann, contribution to this volume

[38] P. Senger, contribution to this volume

[39] G.E. Brown and M. Rho, Phys. Rev. Lett. 66 (1991) 2720

[40] T. Hatsuda and S. H. Lee, Phys. Rev. C 46 (1992) 34

[41] R. Porter *et al.*, Phys. Rev. Lett. 79 (1997) 1229

[42] G. Agakichiev *et al.*, Phys. Rev. Lett. 75 (1995) 7 and Phys. Lett. B422 (1998) 405

[43] E.L. Bratkovskaya *et al.*, Nucl. Phys. A619 (1997) 413

[44] R. Rapp *et al.*, Nucl. Phys. A617 (1997) 472

[45] W.K. Wilson *et al.*, Phys. Rev. C57 (1998) 1865

[46] C. Ernst *et al.*, Phys. Rev. C58 [1998) 447

[47] F. D. Berg *et al.*, Phys. Rev. Lett. 14 (1994) 977

[48] R. Holzmann *et al.*, Phys. Rev. C56 (1997) R2920

[49] J. Friese, contribution to this volume

[50] V. Metag, π-N Newsletter 11 (1995) 159